Universitatea POLITEHNICA din București

Author: Eng. dipl. Vasile AVRAM

PhD THESIS ABSTRACT

INGINERIA SI MANAGEMENTUL OBȚINERII SI PROCESARII ALIAJELOR ANTIFRICȚIUNE INOVATIVE

/

ENGINEERING AND MANAGEMENT OF OBTAINING AND PROCESSING INNOVATIVE ANTI-FRICTION ALLOYS

EVALUATION BOARD OF THE PhD THESIS

President	Prof.univ.dr.ing.Florin MICULESCU	University POLITEHNICA of Bucharest
Scientific Coordinator	Prof.univ.dr.ing.ec Augustin SEMENESCU	
Scientific Referee	Prof.univ.dr.ing. Rodica ION	University “VALAHIA” of Târgoviște
Scientific Referee	Prof.univ.dr.ing.ec. Laura BACALI	Technical University of Cluj-Napoca
Scientific Referee	Prof.univ.dr.ing. Nicolae CONSTANTIN	University POLITEHNICA of Bucharest

- 2022 -

Table of Contents

INTRODUCTION

During their lifetime, all anti-friction materials are repeatedly or occasionally exposed to a number of destructive factors in the environment. These destructive factors can act individually or simultaneously so that the structures of the anti-friction materials change gradually and irreversibly. The implications of these changes lead to a decrease in the performance of anti-friction materials to the point where they can never be used. Anti-friction materials can be used either as individual products or as components of unprotected devices in the environment.

Regardless of the situation, the anti-friction materials undergo destructive processes over time. Due to this aspect, it is necessary to accumulate and deepen the knowledge related to the structure and characterization of anti-friction materials in order to be able to intervene effectively in the processes of stabilization and evaluation of their life (life-time prediction). An in-depth knowledge of these aspects is also of practical use for the correct planning of the maintenance of equipment made of anti-friction materials and its scientific argumentation. Thus, it is necessary to accumulate advanced knowledge on, which has concerned me since the faculty. I would also consider mentioning that I graduated from the Faculty of Metallurgy of the Bucharest Polytechnic Institute, Mineralogy department in 1984 and since graduating until now I have carried out my professional activity in the metallurgical field.

In 2013 I started the company SC MELBA METALURGICAL SRL which deals with the production and sale of YSn83 and YPbSn10 anti-friction alloys. In order to obtain these alloys, we have a good collaboration with the National Institute for Research and Development of Non-Ferrous and Rare Metals - IMNR. The company addresses certain industrial segments such as: railway, cement industry, energy industry, etc. We also managed to export YPbSn10 alloy to Germany. In order to distance ourselves from the competition, we have identified in our concerns a possibility to improve the two alloys, YSn83 and YPbSn10. In this regard, 2 Patents were submitted to OSIM.

PART I THE ENGINEERING FOR OBTAINING AND PROCESSING INNOVATIVE ANTI-FRICTION ALLOYS

Chapter 1. CURRENT STATE OF ANTI-FRICTION ALLOYS

1.1. The role of anti-friction alloys. Functional requirements

The alloys used in the manufacture of bearings are also known as anti-friction alloys. The bearings are the machine parts on which the spindles rests, of particular importance for all categories of machines and mechanisms (engines, machine tools, etc.). The sliding surfaces take over the radial, axial or combined forces of the shaft, allowing it to rotate or oscillate. The great diversity of machines and mechanisms requires different types of bearings, varied both in terms of construction and in terms of materials execution.

An important group of antifriction materials is the one consisting from a soft mass (matrix) with hard inclusions. The representative alloys being the bearings compositions with high content of tin, respectively of lead

The main objective of this paper is represented by the studies and research on the microalloying of antifriction alloys based on tin (Y-Sn83 alloy) and lead (Y-PbSn10), with a number of elements to improve their structure and properties. The topic is multidisciplinary, requiring theoretical knowledge of materials engineering (development of non-ferrous alloys), physico-chemical and structural analysis, strength of materials and tribology, allowing own contributions in the field of anti-friction alloys, effective applications and finished products (lining, bearings, etc.).

The walls of the friction couples (spindle - bearing) must withstand the complex action of lubricating factors by the nature and characteristics of their materials. Because of this, several types of materials, also called antifriction materials, allow solving on a case-by-case basis, under the most favorable conditions, the problems related to the construction of friction couples [1-3].

1.2. Anti-friction alloys based on Sn and Pb

Anti-friction alloys based on tin or lead are considered among the best metallic materials for bearings, being characterized by different methods [3, 5, 6].

The anti-friction alloys based on tin and lead also contain a series of other elements such as: Sb, Cu, Ca, Li, Sr, Ba, Mg etc. [5, 6, 14, 16]

They are generally used as deposited on a layer of bronze or steel by centrifugal casting, as they do not have high mechanical properties. Obtaining these alloys involves choosing the correct chemical compositions and casting conditions, conditions that allow the formation of hard constituents, evenly distributed and intimately integrated into the metallic base mass.

1.2.1. Y-Sn83 tin alloy

The oldest tin-based anti-friction alloys have been known since the early 19th century, consisting of Sn and Sb. The current alloys in this category date from 1839, being also called "babbitt" after Babbitt, who proposed for the first time the following chemical composition: 89.5% Sn, 8.8% Sb and 1.7% Cu. According to this basic formula, a series of variants were created, depending on the structural, metallurgical and technological effects, the deficient material savings, etc. [3, 13, 15,16]

1.2.2. Y-PbSn10 Alloy

The soft matrix of the structure can be obtained from a lead alloy, which has mechanical properties similar to tin. Antimony and tin are commonly used to obtain the hard phases. Hard inclusions can also be obtained with the help of As, Cd, alkaline and alkaline-earth elements such as: Ca, Ba, Na, K [3, 5, 6, 24]

In Romania, the following anti-friction Pb alloys are standardized:

Y-PbSn10: Sn: 10 %, Sb: 15% , Cu: 1%, Pb – balance;

Y-Pb98 : Ca: 0,7%, Na: 0,7% , 0,3% Mg , Pb – balance.

Having mechanical properties similar to those of Y-Sn83 alloy, the anti-friction material Y-PbSn10 is mainly used in the form of a thin layer (0.5-1.0 mm) applied on steel housings in the manufacture of bearings and linings for some types of engines. According to its chemical composition, Y-PbSn10 is a quaternary alloy, in which the alloying elements are antimony and copper: 9.5-12% Sn, 14.5-16.5% Sb, 0.5-1.5% Cu, and Pb. From the structural point of view, the Y-PbSn10 alloy is formed from a relatively soft matrix, consisting of the binary eutectic $\alpha + \beta$, in which the ternary or binary solid solution of lead α is the phase with the lowest hardness. The ternary eutectic phase appears in the matrix $\alpha + \beta + \delta$, shaped as small lines. The actual hard constituents of the alloy are the defined compounds SnSb and Cu_2Sb, both in primary crystallization phases.

1.3. Tendencies regarding the antifriction alloys globally

Literature presents some antifriction metallic materials for the alloys of interest. Nowadays, in addition to the new materials processing technologies, it is practiced to obtain a basic part of the necessary material and then to apply the necessary coatings to improve the properties of its surface [40]. This approach ensures that the surface properties of the resulting product are obtained, extending its functionality [41], resulting in hybrid materials. At the same time, the research carried out during this doctoral thesis has the purpose of filling the gaps currently existing in the literature on antifriction alloys and their microalloying in order to improve their properties.

Chapter 2. IMPROVING THE CHARACTERISTICS OF ANTI-FRICTION ALLOYS BASED ON TIN AND LEAD BY MICRO-ALLOYING

2.1. Methods for improving the properties of anti-friction alloys

The following methods are recommended in the literature to improve the antifriction characteristics of Sn and Pb-based alloys [1-4]:

a. minimizing the content of impurities (in the case of YSn83 alloy - minimizing especially the Pb content);
b. optimizing the basic composition of alloys;
c. microalloying.

Minimizing the content of impurities in anti-friction alloys

Pb present in Y-Sn83 tends to precipitate and cover the crystals of SbSn compound, leading to a decrease in their strength. Lead also forms a eutectic with Sn and Sb with a melting point of 183°C. If the alloy contains Cd (as an alloying microelement), a Pb-Cd eutectic with a melting temperature of less than 145°C is formed.

Optimization of the basic composition of alloys

By varying the content of the alloying elements, within certain limits, contained in the standardized compositions, some technical properties can be further improved: resistance to compression, wear, corrosion, workability by cutting, etc.

Microalloying - One of the most commonly used methods to improve the technical characteristics of anti-friction alloys is microalloying.

2.2. The influence of microalloying elements on the alloy structure

In many cases, the metal melts are subjected, before casting, to thermal treatments, in order to change the solidification conditions, resulting in improved structures and mechanical behavior of the obtained products [4-9].

2.2.1. The effect of microalloying elements in Sn and Pb anti-friction alloys

Microalloying elements / modifiers in tin and lead-based anti-friction alloys have the following effects [4-6]:

Arsenic - Acts as a nucleating agent (germination) for refining SbSn crystals.

Nickel - Ni as a microalloying element has been detected exclusively in Cu_6Sn_5 crystals. The only possible effect of Ni, which due to the small amounts used can be neglected - is increasing the strength due to the mixture of Cu_6Sn_5 crystals.

Cadmium - It is used to increase the strength the alloy matrix, which leads to increased compressive strength.

2.3. Raw materials and equipments used for obtaining Y-Sn83 and Y-PbSn10 microalloyed alloys

The study of obtaining YSn83 and YPbSn10 alloys by rare earth microalloys is the subject of this chapter. The alloys development was carried out by using the metal alloys and composite materials production equipment, according to the invention Patent RO132816-B1.

2.3.1. Prime materials. Used equipment's

The raw materials and materials used in the experimental works for the development of anti-friction alloys are: Sn, Sb, Cu and Pb.

Master alloys

In addition to base metals and pre-alloys, Cu-Sb and Pb-Sb were used in the development of the anti-friction alloys in the considered systems.

2.3.2. Development of YSn83 and YPbSn10 anti-friction alloys

The anti-friction alloys YSn83 and YPbSn10 were obtained in the installation described above using the parameters that will be presented in this section. I decided to make small quantities in order to be able to perform the necessary experiments and to study the effectiveness of the proposed method. Therefore, the amount of YSn83 and YPbSn10 alloys developed: ≈ 100 g/load.

Material loses produced by burning (combustion) will be taken in consideration in the intervals presented in the following table.

Table 2.5. Loss of metals by combustion in the production of tin and lead alloys

Elements	Sn	Pb	Cu	Sb	Mn
%	0,5…1	0,5…1	0,5	0,5	5…10

2.4.2.1.Development of Y-Sn83 antifriction alloys

Încărcătura este compusă din următoarele materiale:

Elements	Master alloy CuSb50	Sb	Sn	Coal
g	**12,2**	**5,0**	**84,0**	**10**

2.4.2.2.Development of Y-PbSn10 anti-friction alloys

The load is composed from following materials:

Elements	Master alloy CuSb50	Master alloy PbSb50	Sn	Pb	Coal
g	**2,2**	**29,0**	**11,2**	**59,0**	**10**

In the following chapters we will describe the microalloying of the basic alloys with several elements and we will analyze the obtained results.

Chapter 3. MICRO-ALLOYING OF ANTI-FRICTION ALLOYS BASED ON TIN AND LEAD WITH MISHMETAL. CASE STUDY.

3.1. Microalloyed alloys development

I decided to microalloy antifriction alloys with mischmetal. Mischmetal was chosen to study the effect it has on the microstructure and properties of selected antifriction alloys. Mischmetal has the composition described in the table 3.1.

Table 3.1. The composition of the mischmetal used in experiments

Element	Ce	La	Nd	Pr	Sm	Yt	Fe, Si, P (sum)	Others (sum):
[% gr]	Bal. (53,8)	24,5	11,4	5,6	1,8	1,5	1,4	< 0,1

*others: Sc, Ca, Ba, Al

For the elaboration of the YPbSn10 alloy microalloyed with mischmetal, the materials are loaded in the following order: copper-antimony pre-alloy, antimony and 2/3 of the total amount of lead. The loaded materials are covered with a layer of dry coal. After melting the charge and overheating the alloy to a temperature of 600-700°C, remove the slag, oxides and unburned coal from the surface and charge the remaining lead and finally the amount of tin. After mixing, the alloy is kept for 10-15 minutes, stirred again and poured at a temperature of 500-550°C into a metal shell. The load is made of the following materials:

Element	Master Alloy CuSb50	Master Alloy PbSb50	Sn	Pb	Master Alloy PbMm10
g	**2,2**	**29**	**11,2**	**48**	**11,2**
Pb-Mm	Melting in quartz crucible * in induction under the atmosphere of dry and purified air (< 5 ppm O_2, H_2O), la 800^0C [3] Load: 18 g Pb, 2 g Mm				9,25…9,75 % ≈ 10 % Mm (sum TR)

For microalloys, the experiments were performed as for the YPbSn10 alloy. After loading the remaining lead and the amount of tin, for a holding time of 10-15 min., PbMm pre-alloy was added, mixed for 1-2 min. and poured at a temperature of 500-550°C in the metal shell.

3.2.Metallographic analysis of elaborate anti-friction alloy samples

3.2.1. Metallographic analysis of YSn83 alloy samples

The developed alloys were chemically analyzed and the results of the chemical analysis are presented in the table. 3.4.

Table 3.4. Determined chemical composition of the analyzed samples

Sample	**Mm[%wt]**	**Sn**	**Cu**	**Sb**	**Pb**	**Zn**	**Fe**	**Al**	**Mm**	**Others***
YSM 1	0,1	bal	6,03	11,34	0,02	<0,01	0,01	<0,01	0,09	<0,01
YSM 2	0,2	bal	5,97	11,68	0,01	<0,01	0,01	<0,01	0,18	<0,01
YSM 3	0,5	bal	5,88	11,08	0,01	<0,01	0,01	<0,01	0,48	0,02
YSM 4	1,0	bal	5,96	10,85	0,02	<0,01	0,02	<0,01	0,93	0,02

Figure 3.1 presents the microstructure of the base alloy YSn83. We observe a structure consisting of Cu_6Sn_5 needles or blades and SnSb cubes embedded in a mass of ternary eutectic consisting of α solid solution, Sn and the intermetallic compound Cu_4Sn [4]. Figure 3.2 shows the base alloy, YSn83, at a higher magnification to highlight the cuboid compound Cu_4Sn. In figure 3.3., the microstructure of the YSM1 alloy is presented in which the Cu_6Sn_5 phase intertwined in the SnSb cuboids can be observed. The mass of the eutectic ternary consisting of solid solution α Sn (Sb) is still visible.

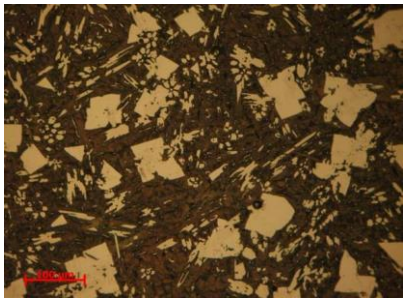

Fig.3.1. Microstructure of cast YSn83 alloy (200 ×)

Fig. 3.2. Microstructura aliajului YSn83 turnat (900 ×)

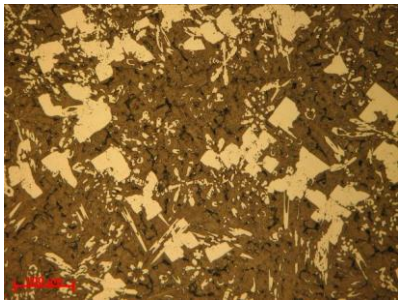

Fig.3.3. YSM1 alloy microstructure (200 ×)

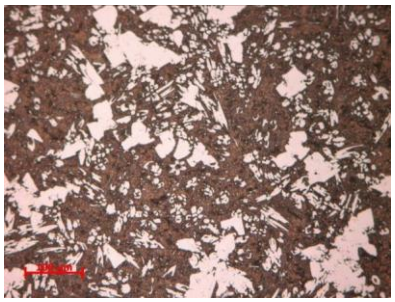

Fig. 3.4. YSM2 alloy microstructure (200 ×)

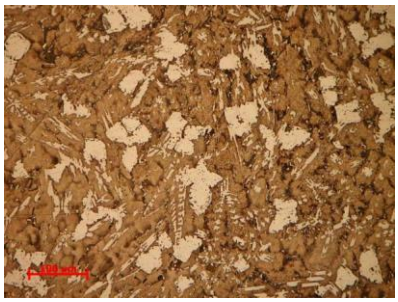

Fig. 3.5. YSM3 alloy microstructure (200 ×)

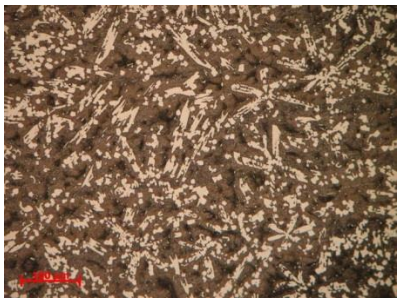

Fig 3.6. YSM4 alloy microstructure (200 ×)

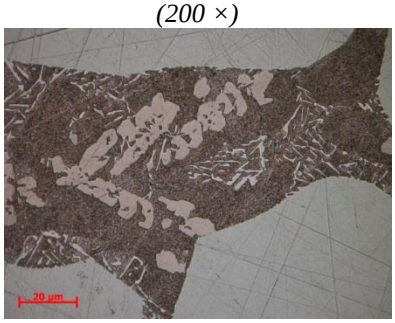

Fig 3.7. YSM4 alloy microstructure (900 ×)

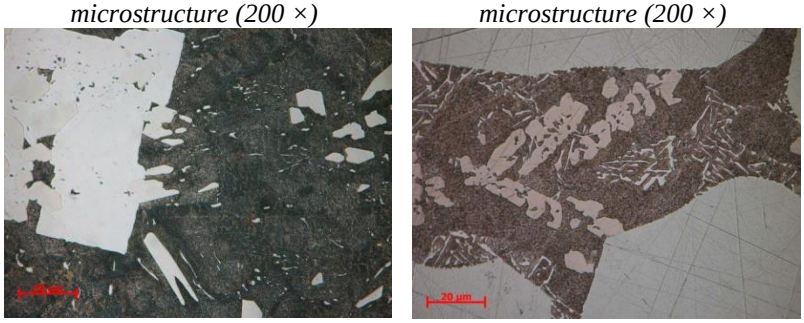

Fig. 3.8. Evolution of the microstructure of the base alloy (a) and the YSM4 microalloy alloy (b)

Figure 3.5 and 3.6 show the sample microstructures of YSM3 and YSM4 in which the acicular crystals of Cu_6Sn_5 compound are highlighted. White, square crystals of SbSn compound were no longer highlighted in these two microstructures. Figure 3.7 shows a detail of the microstructure of the YSM4 sample, with the highest mischmetal content. Figure 3.8 shows a detail of the evolution of the microstructure from the base alloy to the microalloy with 1% mischmetal. The modified structure can be observed as well as the absence of cuboid compounds of SnSb type.

3.2.2. Metallographic analysis of YPbSn10 alloy samples

The developed alloys were chemically analyzed and the results of the chemical analysis are presented in Table 3.5.

Table 3.5. Determined chemical composition of the analyzed samples

Sample	Mm [%wt]	Pb	Sb	Sn	Cu	Zn	Fe	Al	Mm	Others*
YPM 1	0,1	bal	6,03	11,34	0,93	<0,01	0,01	<0,01	0,09	<0,01
YPM 2	0,2	bal	5,97	11,68	1,08	<0,01	0,01	<0,01	0,21	<0,01
YPM 3	0,5	bal	5,88	11,08	0,92	0,02	0,02	<0,01	0,49	0,02
YPM 4	1,0	bal	5,96	10,85	1,12	0,01	0,02	<0,01	1,05	0,03

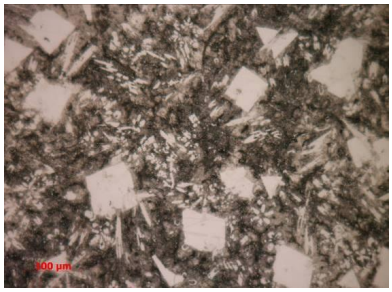

Fig. 3.9. Microstructure of cast YPbSn10 alloy (200 X)

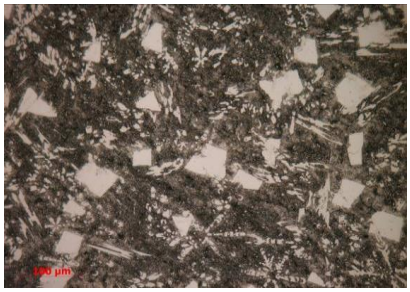

Fig 3.10. YPM1 alloy microstructure (200 ×)

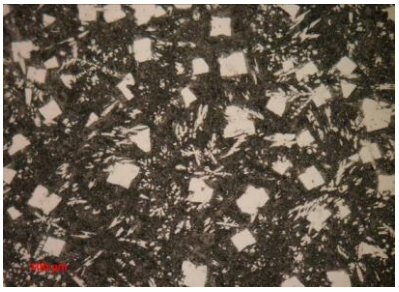

Fig. 3.11. YPM2 alloy microstructure (200 ×)

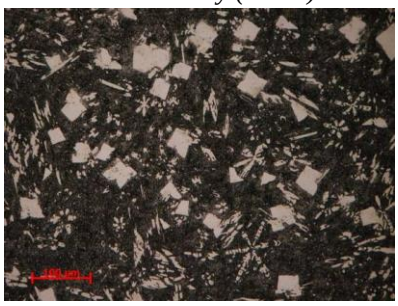

Fig 3.12. YPM3 alloy microstructure (200 ×)

Fig 3.13. YPM4 alloy microstructure (200 ×)

Fig.3.15. YPM4 microalloyed with 1.0% Mm (900 ×)

The structure is composed of Cu_2Sb rods and needles and SnSb cubes embedded in a mixture of binary and ternary eutectic phases, which form the soft matrix of the alloy. Figure 3.10 shows the first changes. The alloy matrix shows a decrease in cuboids and the appearance of lamellar structures and strings of compounds.

3.3 Mechanical characterization of anti-friction alloys alloyed with mischmetal

The Brinell hardness of the developed anti-friction alloys was determined by using a WPM hardness tester model HPO 3000, Germany. The measurements were performed under the following conditions:

Force [daN]	D [mm]	Ment. [s]	Temp. [ºC]
250	10	60	20 , 50±1 , 100±2

In Fig. 3.17 and Fig. 3.18 diagrams with the variation of the hardness of the anti-friction alloys depending on the content of the microalloy element are presented.

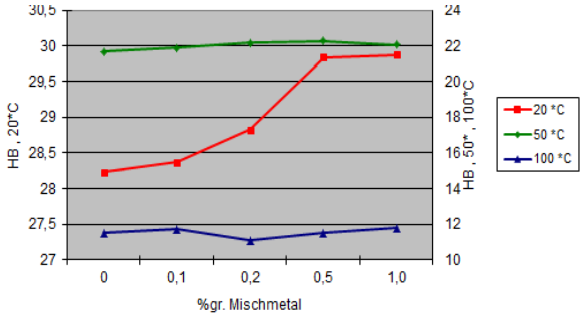

Fig. 3.17. Hardness of YSn83 microalloyed alloys

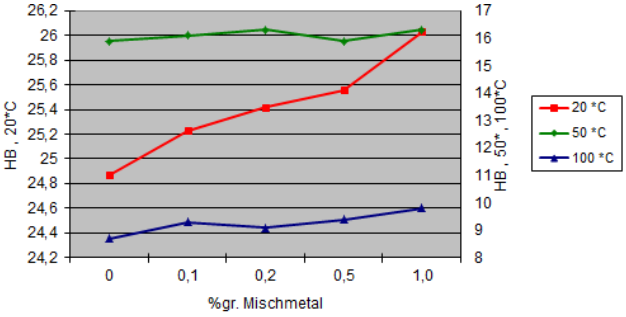

Fig. 3. 18 Hardness of microalloyed YPbSn10 alloys

3.4 *C*ompressive strength determination

The dynamic compressive strength of YSn83 and YPbSn10 alloys was determined by the discharge method.

The variation of the compressive strength of the Y-Sn83 and Y-PbSn10 alloys depending on the content of the microalloy element is shown in Fig. 3.19 and Figs. 3.20.

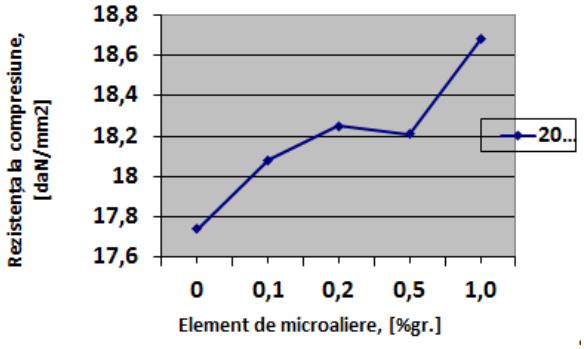

Fig. 3.19. Compressive strength of Y-Sn83 microalloyed alloys

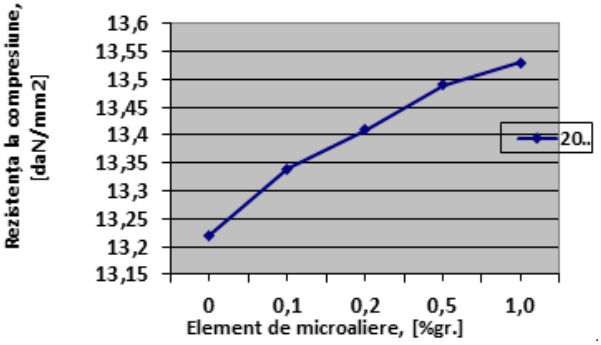

Fig. 3.20. Compressive strength of microalloyed YPbSn10 alloys

The increase in the dispersion of the hard phase in the soft matrix of the alloys can be the consequence of the increase of the HB hardness of the alloys by 3 - 5% and of the compressive strength by 3 - 6%.

As the temperature increases, the hardness decreases, as a consequence of possible recrystallization phenomena that occur during the heating of the samples - it is known that Sn and Pb alloys have relatively low recrystallization temperatures.

Chapter 4. MICRO-ALLOYING OF ANTI-FRICTION ALLOYS BASED ON TIN AND LEAD WITH CALCIUM AND MAGNESIUM

4.1. Chemical analysis of elaborated alloys

Ca and Mg microalloyed YSn83 alloys were obtained by using the same working method as for the mischmetal alloyed YSn83 alloys. This way of working was presented in detail in chapter 3, subchapter 3.1.

In order to reduce the cost price of tin-based anti-friction alloys, some of the tin is replaced by lead, making Quaternary Sn-Pb-Sb-Cu alloys. Alloys with a lower tin content are usually hardened by the addition of other elements, which form intermediate phases, such as: As, Cd, Te, Ni. By adding As, Cd or Te forms new hard constituents, which improve the antifriction properties of the alloys and allow the reduction of the Sb content. These alloys have been proposed for patenting [1].

The calculated composition of YSn83 alloy microalloyed with Ca and Mg respectively is shown in Table 4.1.

Table 4.1. The composition of the YSn83 alloy microalloyed with Ca and Mg respectively

Alloy brand	Chemical Composition % gr.								
	Sn	Sb	Cu	Pb	Al	Mg	Ca	Other Elements	Impurities
Y-Sn83Ca	82-84	10-12	5,5-6,5	-	-	-	0,2-0,5	-	0,25
YSn83Mg	82-84	10-12	5,5-6,5	-	-	0,2-0,5	-	-	0,25

YPbSn10 microalloyed alloys with Ca and Mg were obtained by the same method as YPbSn10 microalloyed alloys with mischmetal. The method of production and the equipment used are described in detail in Chapter 3, Subchapter 3.1. Development of microalloyed alloys. Table 4.2 shows the compositions calculated for the YPbSn10 alloy microalloyed with Ca and Mg, respectively.

Table 4.2. The composition of the YPbSn10 alloy microalloyed with Ca and Mg

Alloy Brand	Chemical Composition % gr.								
	Sn	Sb	Cu	Pb	Al	Mg	Ca	Other Elements	Impurities
YPbSn10Ca	9,5-12	14,5-6,5	0,5-1,5	Rest	-	-	0,2-0,5	-	Max 0,2
YPbSn10Mg	9,5-12	14,5-6,5	0,5-1,5	Rest	-	0,2-0,5	-	-	Max 0,2

The following notations, presented in Table 4.3, were further used to identify the evidence.

Table 4.3 Notations used to identify samples

Alloy Name	Sample Alloy
YSn83	YS0
YSn83Ca0,2	YS1
YSn83Mg0,2	YS2
YPbSn10	YP0
YPbSn10Ca0,2	YP1
YPbSn10Mg0,2	YP2

4.1.1. Metallographic analysis of the anti-friction alloy samples

4.1.2. YSn83 Metallographic analyses results

The developed alloys were chemically analyzed and the results of the chemical analysis are presented in the table. 4.4.

Table 4.4. Determined chemical composition of the analyzed samples

Sample Name	**Sn**	**Cu**	**Sb**	**Pb**	**Zn**	**Fe**	**Al**	**Ni**	**Mo**	**Ca**	**Mg**	**Others***
YS1	base	6,9	11	0,44	<0,02	<0,02	<0,02	<0,02	<0,02	0,22	-	<0,01
YS 2	base	6,32	10,7	0,46	<0,02	<0,02	<0,02	<0,02	<0,02	-	0,23	<0,01

Figure 4.1 shows the microstructure of the base alloy YSn83. We observe a structure formed by needles or lamellae of Cu_6Sn_5 and of SnSb cubes embedded in a mass of ternary eutectic formed by solid solution α, Sn and the intermetallic compound Cu4Sn [3]. Figure 4.2 shows the microstructure of the YS1 sample in which we can see hard CaSn3 compounds evenly distributed in the alloy matrix. Calcium forms hard CaSn3 compounds and has low toxicity. Magnesium also forms the compound $MgSn_2$, a hard compound and also has low toxicity. These elements can segregate at the grain (crystal) / dendrite boundaries and by reducing the grain / dendrite interface energy, it slows down the movement or sliding of the borders. In addition, they can help remove impurities (such as sulfur, phosphorus, etc.), change the properties, shape and distribution of inclusions, and thus improve the technological properties of alloys.

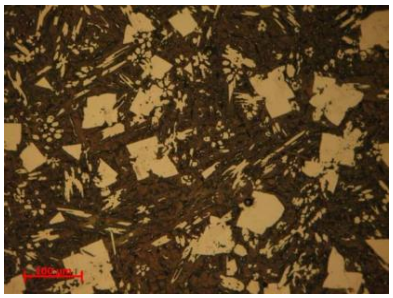

Fig.4.1. Microstructure of cast YS0 alloy (200 ×)

Fig. 4.2. YS1 sample microstructure (100x)

Fig. 4.3. YS2 sample microstructure (100x)

In the YS2 sample, microalloyed with magnesium, the hard compound $MgSn_2$ and a fine lamellar eutectic can be observed, evenly distributed in the whole matrix of the basic

alloy. In the electron microscopy analyzes that will be presented. We also identified the compound that appears in this optical microstructure.

4.1.3. Metallographic analysis of YPbSn10 alloy samples

The elaborated alloys were chemically analyzed and the results of the chemical analysis are presented in table 4.5.

Table 4.5. Determined chemical composition of the analyzed samples

Sample Name	**Pb**	**Cu**	**Sb**	**Sn**	**Zn**	**Fe**	**Al**	**Ni**	**Mo**	**Ca**	**Mg**	**Others***
YP1	baza	1,03	13,5	8,7	<0,02	<0,02	<0,02	<0,02	<0,02	0,23	-	<0,01
YP2	baza	1,19	13,9	7,1	<0,02	<0,02	<0,02	<0,02	<0,02	-	0,21	<0,01

Ca and Mg elements for microalloys were chosen for this doctoral thesis. Ca forms hard CaPb3 compounds and has low toxicity. Mg also forms the hard compound MgPb2 and also has low toxicity. These elements can segregate at the grain / dendrite boundaries and by reducing the grain / dendrite interface energy, it slows down the movement or sliding of the grain.

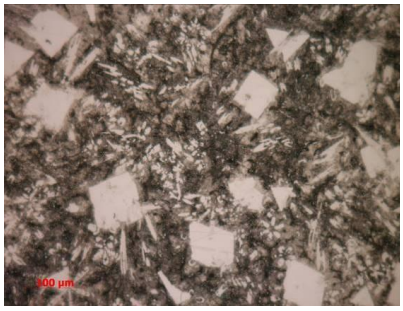

Fig. 4.4. Microstructure of cast YP0 alloy (200 X)

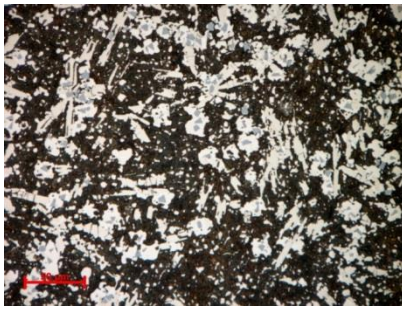

Fig.4.5. Microstructure of the YP1 sample

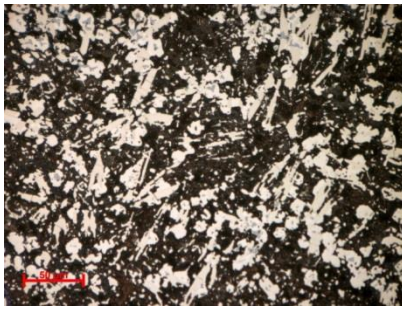

Fig. 4.6. Microstructure of the YP2 sample

The structure consists of Cu_2Sb rods and needles and SnSb cubes embedded in a mixture of binary and ternary eutectic phases, which form the soft matrix of the alloy.

Figure 4.5 shows the microstructure of the YP1 sample and Figure 4.6 shows the microstructure of the YP2 sample. Figure 4.5 shows the microstructure of the sample microalloyed with Ca, homogeneous, with small globular compounds and larger globular compounds, $CaPb_3$ as well as compounds with the needle shape of probably SnSb.

Figure 4.6 shows polyhedral compounds, $MgPb_3$, evenly distributed in the soft matrix of the alloy. SnSb acicular compounds are reduced compared to the calcium microalloyed sample

4.1.3. Microstructural characterization of anti-friction alloys Y-Sn83 and Y-PbSn10 microalloyed with Ca and Mg

The samples were prepared for microstructural analysis. The samples were incorporated into the ProbeMet type resin. The sanding was done on abrasive paper and the polishing on Lecloth type cloth, soaked with a suspension of α-alumina in water. The attack was performed with C_2H_6O solution (ethyl alcohol) + HNO_3 (nitric acid). A high vacuum FEI Quanta 250 microscope, CBS, ESD and BSE was used for analysis. The software used was XT Microscope dedicated server for SEM ELEMENT EDS Analysis Software Suite dedicated for EDS.

The EDS semiquantitative chemical analyzes acquired in specific areas are performed on each individual compound which indicates the following chemical composition:

- the cubic-shaped compound, contains mostly Sb-Sn (fig. 4.9a, 4.14a)
- the needle-shaped compound, contains mostly Cu-Sb-Sn (fig. 4.9b, 4.14b)

Following the EDS / live-map analysis, a distribution of the elements according to each structure was highlighted (fig. 4.10, 4.11 and fig. 4.15, 4.16). In the case of the analyzed Sn alloys, the basic metal mass consists of Sn. The presence of carbon in the EDS analyzes performed can be explained by its presence in the embedding resin used.

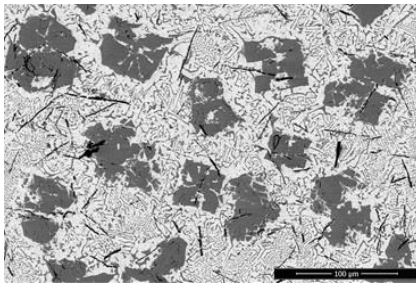

Fig. 4.7. SEM image of YP1 sample obtained with backscattered secondary electron detector (CBS) in High Vaccum mode.

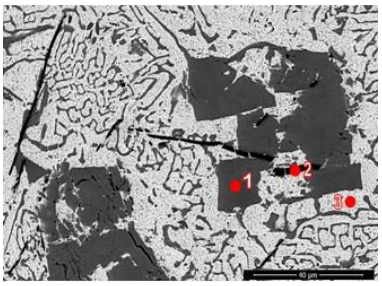

Fig 4.8. SEM image of sample P1, with points selected for EDS analysis,

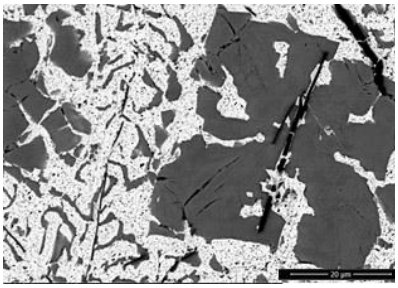

Figura 4.10. SEM image of the YP1 sample with the area selected for EDS / Live-Map analysis

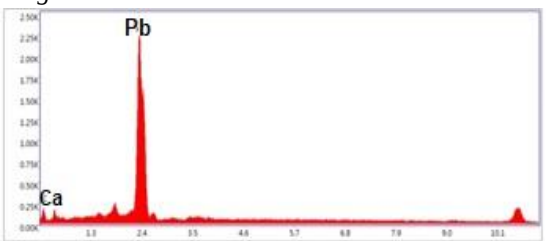

Element	Masa %	Atm. %	Net Int.
Ca K	8.99	63.02	57.57
PbM	91.01	36.98	768.33

Fig.4.9. The results of the EDS analysis of sample P1 performed in section 1 referred to in Figure 4.8 (c)

From the EDS results it can be seen that the alloy has lead in the composition, in accordance with the specifications of the initial alloy. The cuboid compound contains CuSnPb and the acicular compound contains CuSnSb and is found in small amounts. Figure 4.10 shows the microstructure of the YP1 sample at a larger magnification to focus the polyhedral compound formed. The image was obtained with the Scattered Secondary

Electron Detector (CBS) in High Vaccum mode. From the mapping performed (fig.4.11) we can see that the composition of the polyhedral compound includes Sn, Sb and Cu and in the acicular compound it is observed that Cu is present in a small amount

Figure 4.10 shows the microstructure of the YP1 sample at a larger magnification to focus the polyhedral compound formed. The image was obtained with the Scattered Secondary Electron Detector (CBS) in High Vaccum mode. From the mapping performed (fig.4.11) we can see that the composition of the polyhedral compound includes Sn, Sb and Cu and in the acicular compound it is observed that Cu is present in a small amount

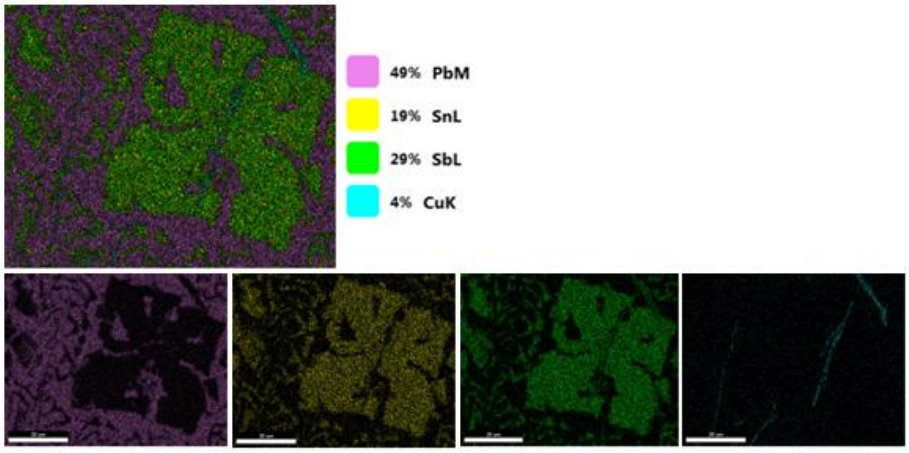

Fig. 4.11. The results of the EDS / Live-Map analysis of the YP1 sample

Figure 4.12 shows the microstructure of sample YP2, microalloyed with magnesium. We can observe a homogeneous lamellar eutectic structure in the whole mass of the sample and cuboidal compounds containing mainly Sn and Sb. Acicular compounds contain Pb, Cu, Sn and Sb. Figure 4.12 shows the microstructure at a larger magnification to highlight the cuboidal compound to perform the EDS analysis of the studied sample. Figure 4.13 shows the EDS analysis of the enlarged sample.

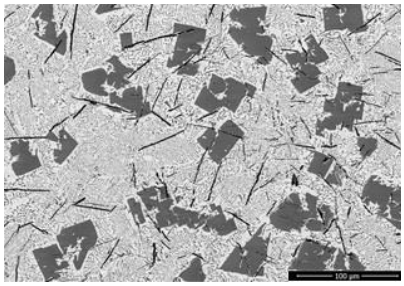

Fig. 4.12. SEM image of sample P2

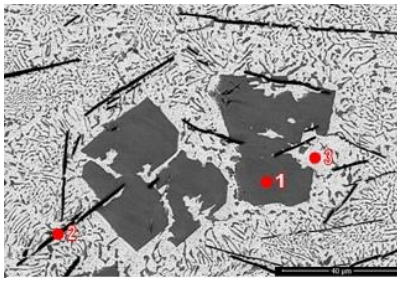

Fig. 4.13. SEM image of the YP2 sample with selected points for EDS analysis

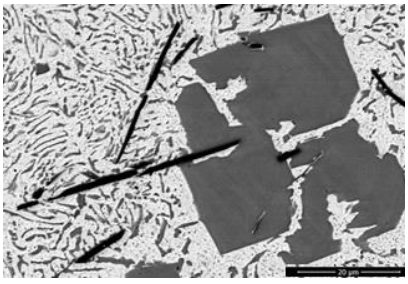

Fig. 4.15. SEM image of sample P2 with selected area for EDS analysis

Figure 4.15 shows the microstructure of the YP2 sample and the mapping performed on this sample. We can see from the presented images that in the cuboidal compound we find mainly Sb and Sn, with a small amount of Cu. The acicular compound contains Sb and Cu and the matrix is predominantly Pb. The compound MgPb2 is the fine eutectic that appears in the mass of Pb. It is the hardest compound evenly and homogeneously distributed in the analyzed microstructure.

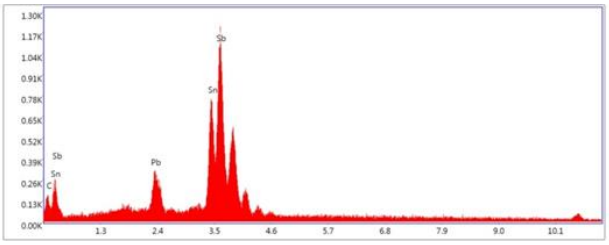

Elemen	Wt %	At %	Net Int.
C K	3.08	24.97	38.66
PbM	9.30	4.36	82.86
SnL	34.84	28.53	289.38
SbL	52.78	42.14	404.87

Fig. 4.14. Results of the EDS analysis of the YP2 sample performed in point 1

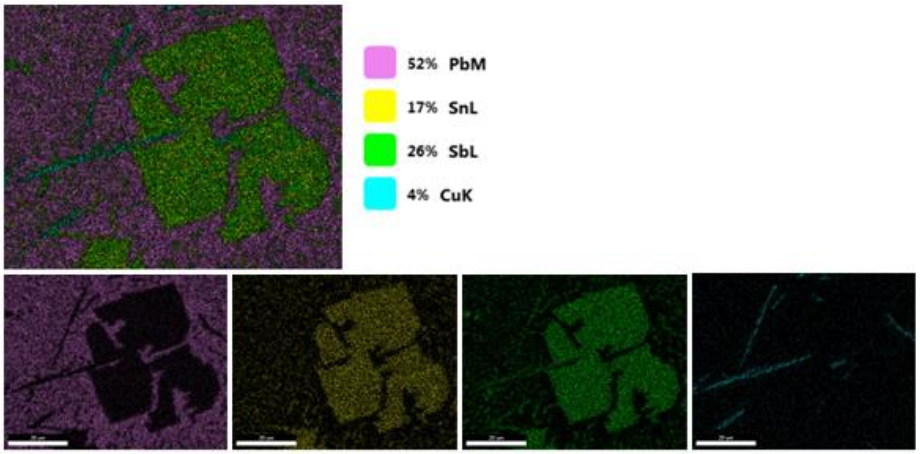

Fig. 4.16. Results of the EDS / Live-Map analysis of the YP2 sample..

Figure 4.17 shows the high vacuum mode, the image being obtained with scattered electrons. We observe the soft matrix of the light gray alloy (point 4 corresponding to figure 4.18 in which we present the microstructure on which the EDS analysis of the YS1 sample was performed. In the acicular-cylindrical phase dark gray was identified the presence of Sb and Cu and in the area marked with 3 was identified the presence of Cu, Sn and Sb probably forming the compound SnSbCu.

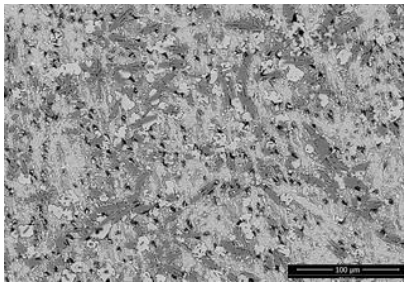

Fig. 4.17. SEM image of the YS1 sample

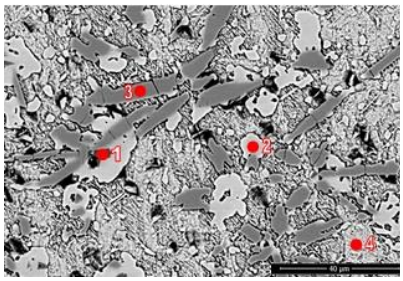

Fig. 4.18. SEM image of P3 sample

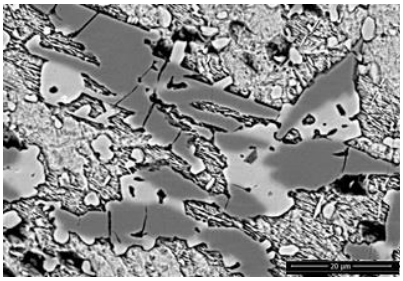

Fig. 4.19. SEM image of YS1 sample

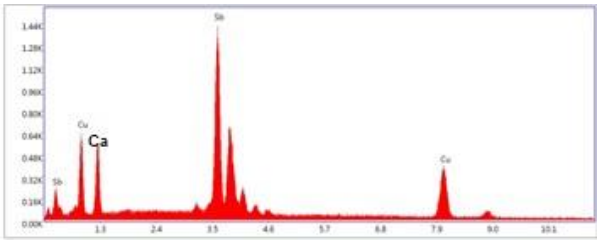

Element	Weight %	Atomic %	Net Int.
CaK	13.06	36.98	161.16
SbL	60.24	34.08	591.07
CuK	26.70	28.94	213.49

Fig. 4.20. The results of the EDS analysis of the YS1 sample performed in point 1

Figure 4.19. presents the SEM image of the YS1 sample with the area selected for EDS / Live-Map analysis, obtained with the backscattered secondary electron detector (CBS), in High Vaccum mode. Figure 4.21 shows the mapping of the elements present in this microstructure. From the mapping presented we can observe that Ca is evenly distributed in the matrix of Sn, Sb and Cu present in polyhedral compounds and Sb also present together with Sn in the matrix of the base alloy. Calcium forms the compound CaSn3, a harder compound that is evenly distributed in the soft alloy matrix. The compound with Ca is the one that improves the qualities of the formed alloy.

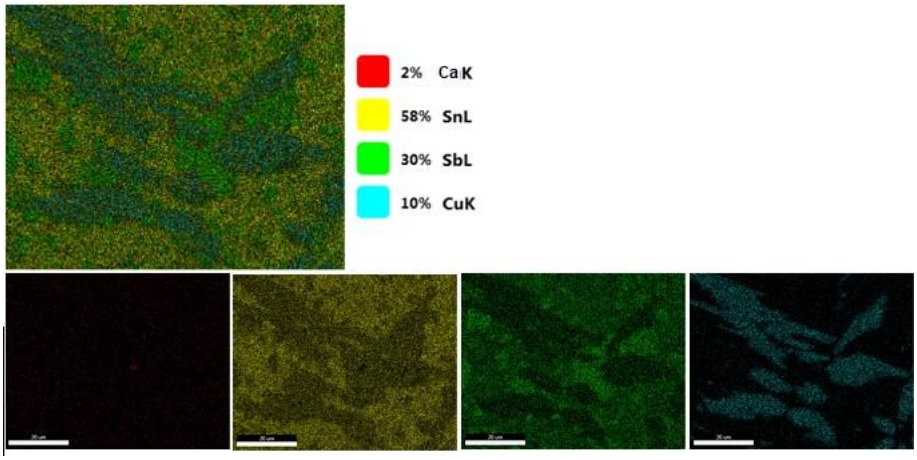

Fig. 4.21. The results of the EDS / Live-Map analysis of the YS1 sample

Figure 4.22 shows the microstructure of the YS2 sample, microalloyed with Mg. A major phase of the alloy with Sn and Sb and some dark gray cylindrical compounds can be seen. There are also light gray and dark gray polyhedral compounds.

Figure 4.23 shows the microstructure of the YS2 sample on which the EDS analysis was performed to identify the component elements. Figure 4.24 a shows the elements identified by the EDS analysis in the points highlighted in Figure 4.23.

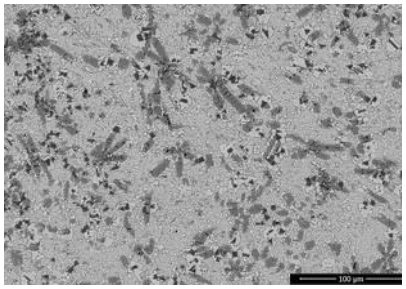

Fig. 4.22. SEM image of the YS2 sample obtained with the backscattered secondary electron detector (CBS) in High Vaccum mode.

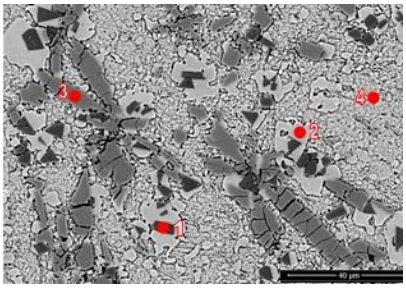

Fig. 4.23. SEM image of the P4 sample with the selected points for EDS analysis, obtained with the backscattered secondary electron detector (CBS), in High Vaccum mode.

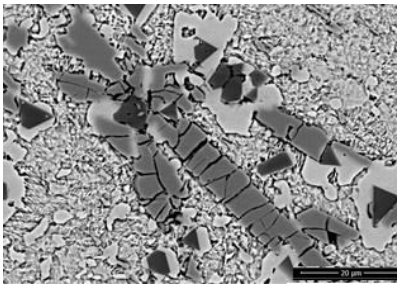

Fig. 4.25. SEM image of the YS2 sample with the area selected for EDS / Live-Map analysis, obtained by Scattered Secondary Electron Detector (CBS)

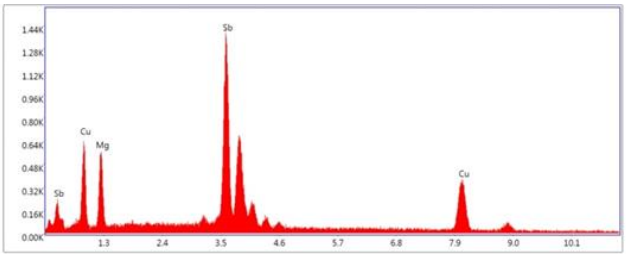

Element	Weight %	Atomic %	Net Int.
MgK	13.51	37.91	168.01
SbL	59.90	33.56	588.64
CuK	26.58	28.53	212.86

Fig. 4.24. The results of the EDS analysis of the YS2 sample performed in point 1 mentioned in Figure 4.23

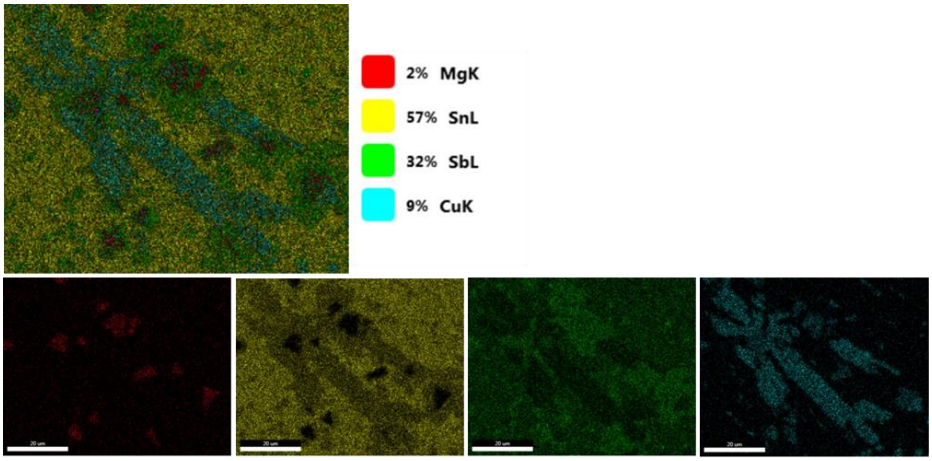

Fig. 4.26. The results of the EDS / Live-Map analysis of the YS2 sample

EDS point semiquantitative chemical analyzes performed on each structure indicate the following chemical composition:

- trigonal form compound, contains mostly Sb-Cu-Mg (fig. 4.19a, 4.23)
- irregular shape compound, contains mostly Sb-Sn (fig. 4.19b, 4.24b)
- acicular-columnar shape compound, contains mostly Cu-Sb-Sn (fig. 4.19c)

4.2.X-ray diffraction analysis of Ca and Mg microalloyed samples

Data acquisition was performed on the BRUKER D8 ADVANCE diffractometer using DIFFRACplus XRD Commender software (Bruker AXS), by diffraction method Bragg-Brentano, cuplaj Θ – Θ

The data processing was performed with the help of the DIFFRAC.EVA VER.5 2019 program from the DIFFRAC.SUITE.EVA software package and the ICDD PDF4 + 2021 database.

Figure 4.27 shows the diffractogram of the YP1 sample in which peaks are identified for the SnSb, PbSnSb and Cu_2Sb phases. Table 4.8 shows the compounds identified in the diffractogram. A smaller peak with the compound $CaPb_3$ can also be observed.

Figure 4.28 shows the diffractogram of the YP1 sample with the quantitative analysis of the analyzed sample. The quantitative analysis was performed using the DIFRAC.EVA release 2019 software and the ICDD PDF4 + 2021 database. Table 4.8 shows the peaks present in figure 4.28.

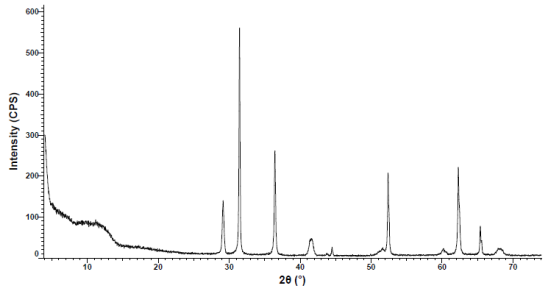

Fig.4.27. YP1 diffractogram (primary data).

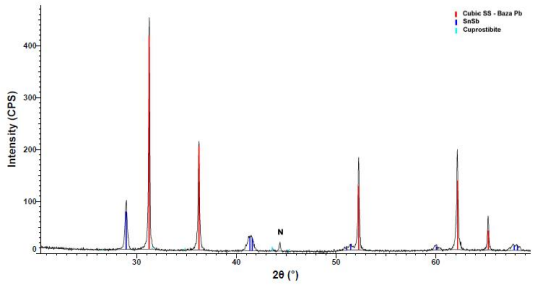

Fig. 4.28. Diffractogram of sample YP1 with Ca content

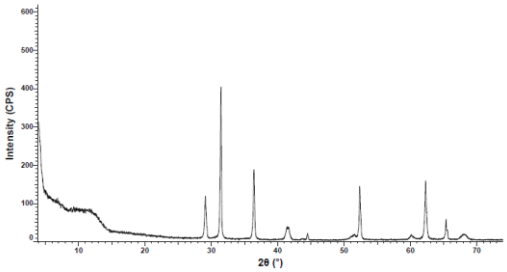

Fig. 4.30. YP2 sample diffractogram, primary data

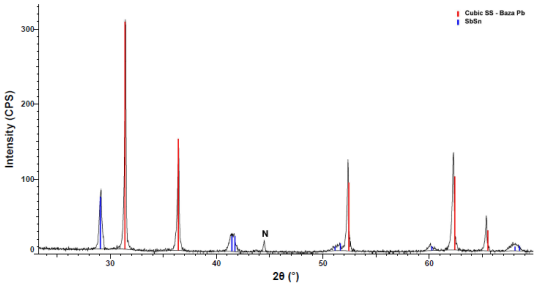

Fig. 4.31. Diffractogram of YP2 sample with quantitative analysis

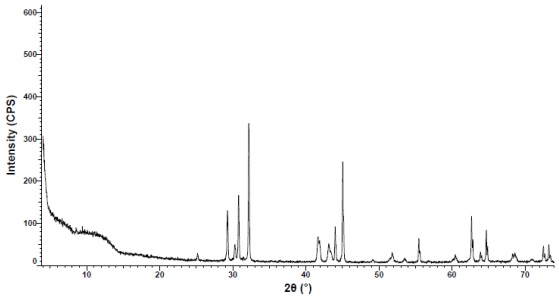

Fig. 4.32. YS1 sample diffractogram (primary data)

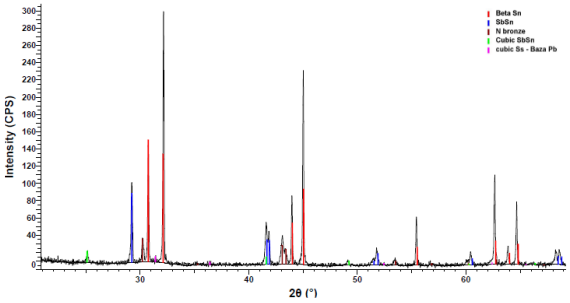

Fig. 4.32. Diffractogram with quantitative analysis of the YS1 sample

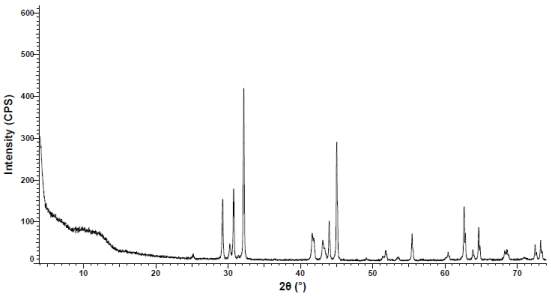

Fig. 4.33. YS2 sample diffractogram (primary data)

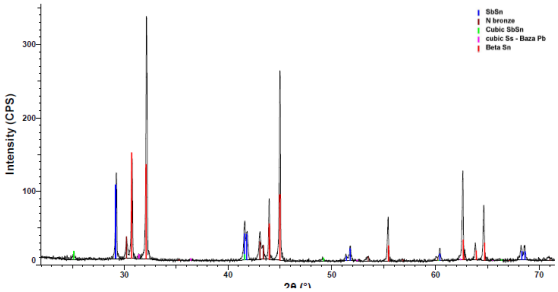

Fig. 4.34. Diffractogram with quantitative analysis of the YS2 sample.

In Figure 4.28 the calcium-containing compound is present at the highest peak in the figure. This identification is consistent with electron microscopy data where the calcium-containing compound is evenly distributed in the soft matrix of the material. In the next chapter we will study the influence that this compound has on the tribological properties of the studied alloy. Figure 4.31 shows the diffractogram for the YP2 sample with quantitative data obtained using the DIFRAC.EVA release 2019 software and the ICDD PDF4 + 2021 database. In figure 4.31 the highest peak is represented by the compound with similar cubic

structure with Mg and Pb. Figure 4.32 presents the diffractogram of the YS1 sample. Notice the different profile from the YP1 and YP2 samples as the alloy base is changed. Figure 4.33 shows the diffractogram with quantitative analysis performed with the same software and databases as in the case of samples YP1 and YP2. Figure 4.34 shows the diffractogram of the YS2 sample with the quantitative analysis performed for the microalloyed alloy with Mg.

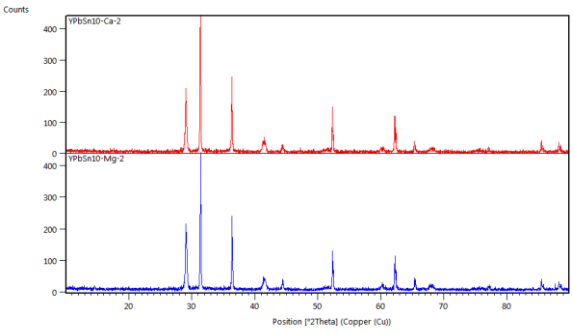

Figura 4.35. Analiza comparativa probelor YP1 și YP2.

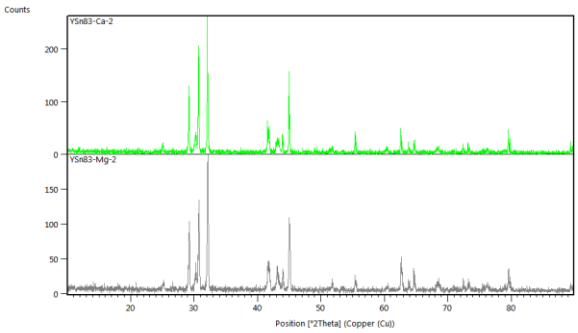

Figura 4.36. Comparație între probele YS1 și YS2

For the YS1 and YS2 samples we can observe a similarity of the diffractograms, the high peak containing Ca for the YS1 sample and Mg for the YS2 sample. Also, the middle peak in the image above, which corresponds to the two diffractograms, is represented by the compound Cu_6Sn_5. Otherwise, there are small differences due to the effect of the microalloy elements used.

In the case of samples YP1 and YP2, the analysis by X-ray diffraction highlights the presence of a majority phase of solid solution type with Pb base, solid substitution solution and a compound with rhombohedral structure SnSb. The analysis also identifies a small percentage of Cuprostibite in the case of the first sample.

In the case of samples YS1 and YS2, the presence of a majority tetragonal structure is observed - associated with βSn.

Chapter 5. TRIBOLOGICAL CHARACTERIZATION OF YSN83 AND YPBSN10 ALLOYS MICROALLIATED WITH CALCIUM AND MAGNESIUM

Alloys obtained by microalloying them with Ca and Mg are mainly used in tribological applications. The experimental determinations presented in the doctoral thesis were performed by using the CETR UMT Multi-Specimen Test System tribometer, from the Department of Machine Parts and Tribology (Faculty of Mechanical and Mechatronics Engineering, Polytechnic University of Bucharest).

The pin-on-disk system was used for the tests presented in this chapter on the UMT II CETR tribometer. This test method involves the use of a pin-shaped specimen mounted on the top of the tribometer, a specimen that slides under a set of predetermined conditions on a flat surface that has a translational motion. The UMT II tribometer allows real-time monitoring of normal load force (Fz), friction force (Ff) and coefficient of friction (COF).

For these tests, the UMT II CETR tribometer was equipped with a two-way force sensor model DFH-20, used to measure the friction force between the upper and lower specimen, as well as to measure and control the normal load force. The upper specimen holder secures the pin to the damping system, while the lower specimen holder secures it to the L20HE translation unit of motion used for these tests. In this case, the pin, which was made of bronze, has a length of 28 mm and a diameter of 6.35 mm, and the lower specimen were represented by the four samples of different materials.

The samples used are summarized in Table 5.1. In order to determine the coefficient of friction between the four materials and the bronze pin, tribological tests of friction with linear motion over a length of 5 mm were performed at three different sliding speeds (0.1 mm / s, 0.5 mm). / s and 1 mm / s) and at three different normal load forces (5 N, 10 N and 15 N). Given that the nominal contact area between the pin and the four samples is a cylindrical area determined by the diameter of the pin, the contact pressure corresponding to the three loading forces was 0.16 MPa (5 N), 0.32 MPa (10 N) and 0.48 MPa (15 N).

Table 5.1. Notations used for sample identification

Alloy Name	Sample Name
YSn83	YS0
YSn83Ca0,2	YS1
YSn83Mg0,2	YS2
YPbSn10	YP0
YPbSn10Ca0,2	YP1
YPbSn10Mg0,2	YP2

The results for the average value of the friction coefficient are centralized in Table 5.2, and the evolution of the coefficient for the 36 tests is presented graphically in Fig.5.2 - 5.37.

Table 5.2. Average value of the friction coefficient

Sample	**Load Force F_z**	**Relative travel speed**		
		0,1 mm/s	**0,5 mm/s**	**1 mm/s**
YP1	**5 N**	0,0871	0,1015	0,0916
	10 N	0,0989	0,1021	0,1074
	15 N	0,1033	0,1126	0,1097
YP2	**5 N**	0,1007	0,1159	0,1286
	10 N	0,0975	0,1153	0,1190
	15 N	0,1013	0,1008	0,1410
YS1	**5 N**	0,0713	0,0663	0,0741
	10 N	0,0832	0,0718	0,0756
	15 N	0,0960	0,0769	0,0813
YS2	**5 N**	0,1051	0,1022	0,1125
	10 N	0,1008	0,0926	0,1094
	15 N	0,1160	0,1256	0,1406

The analysis of the results shows the lowest values of the coefficient of friction were obtained for the YS2 sample. In the case, the increase in the relative slip velocity does not significantly affect the coefficient of friction values. An increase in the normal loading force also leads to a slight increase in the friction coefficient.

Figure 5.2 shows the variation of the friction coefficient, for case of pressing with a normal force of 5N and a speed of 0.1mm / s. There is a relatively constant evolution of the friction coefficient with its average value being 0.0871.

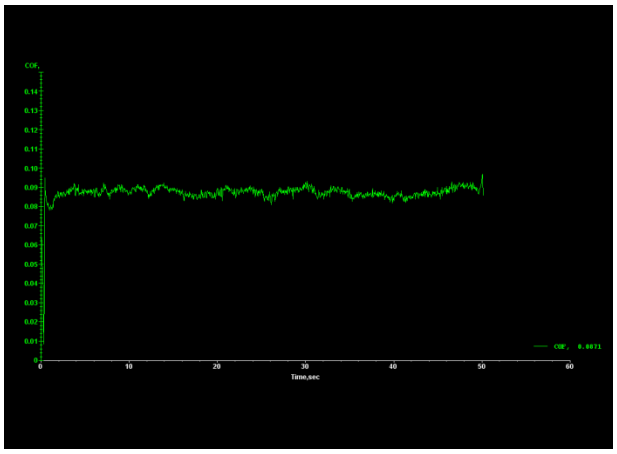

Fig. 5.2. Friction Coefficient Evolution – YP1 (F_z = 5 N, v = 0,1 mm/s)

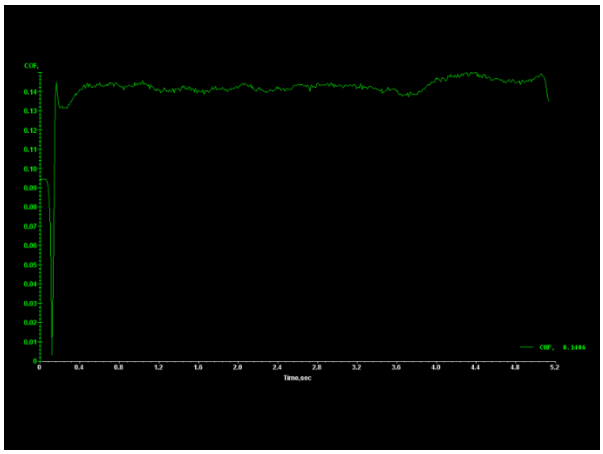

Fig. 5.37. Friction Coefficient Evolution – YS1 (F_z = 15 N, v = 1 mm/s)

The analysis of the obtained results is presented in the following figures.

Figure 5.38 shows the variation of the results obtained for the YP1 test.

It can be seen that the lowest values of the coefficient of friction were obtained for the analyzed sample at a force of 5N and a speed of 1mm / s.

Figure 5.39 shows the variation of the friction coefficient for the YP2 sample.

From the analysis of the obtained results it can be seen that the lowest value was that for the force of 10N at a speed of 0.1mm / s. Figure 5.40 shows the results of the tribological

analysis for the YS1 sample. From the presented image it can be seen that for this test the minimum value obtained for the friction coefficient was obtained for the analyzed sample at a force of 5N and a speed of 0.5 mm / s.

Figure 5.41 shows the results obtained for the YS2 test. It can be seen that for this test the minimum value of the friction coefficient was obtained for the analyzed sample with a force of 10N and a speed of 0.5 mm / s. The analysis of the results shows the lowest values of the friction coefficient were obtained for the YS2 sample. In the case of this test, the increase in relative slip velocity does not significantly affect the friction coefficient values. Only an increase in the normal loading force also leads to a slight increase in the friction coefficient.

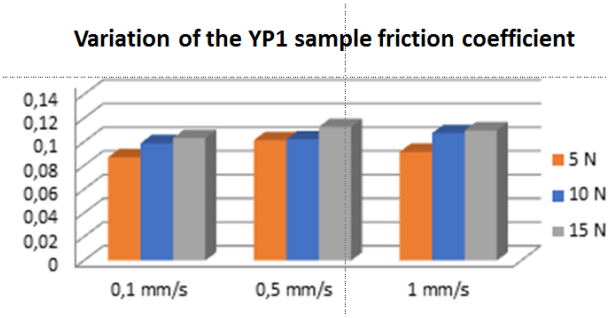

Fig. 5.38. Friction coefficient variation for YP1

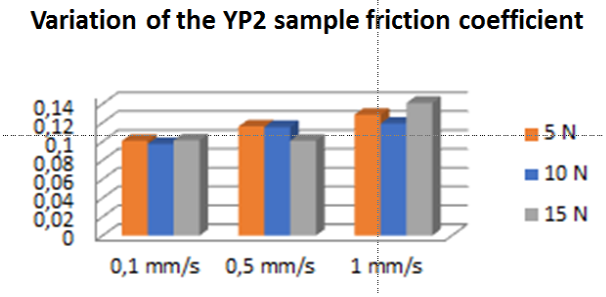

Figura 5.39. Friction coefficient variation for YP2

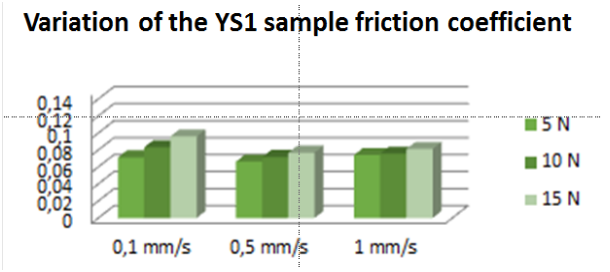

Figura 5.40. Friction coefficient variation for YS1

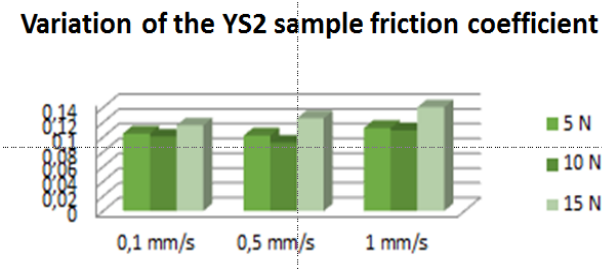

Figura 5.41. Friction coefficient variation for YS2

PART II – PART II - MANAGEMENT OF PRODUCTION AND MARKETING ON THE NATIONAL AND INTERNATIONAL MARKET OF INNOVATIVE ANTI-FRICTION ALLOYS

The elements presented above related to the Vision 2050 for the non-ferrous metals industry, require me, along with the innovative solutions presented in part I of the doctoral thesis, to develop in the second part of the thesis, which includes viable solutions in the field of metals and alloys management. non-ferrous metals, market study, production and cost evolution of non-ferrous metals in order to carry out a business plan and a marketing plan to place on the national and international market, patented anti-friction materials.

Chapter 6. ELEMENTS APPLICABLE TO THE PRODUCTION OF NON-FERROUS ALLOYS MANAGEMENT

This chapter presents the correlations between management functions and enterprise functions. The concepts of efficiency and effectiveness are defined and analyzed. Economic organizations (enterprises) and management are analyzed in this chapter. Thus, the work processes are analyzed within the two categories: execution processes and management processes. It also presents the defining features for managers: multiple professionalization; the accentuated creative (innovative) character of the carried out activities.

6.4. Production process management

6.4.1. Defining production management. Main features.

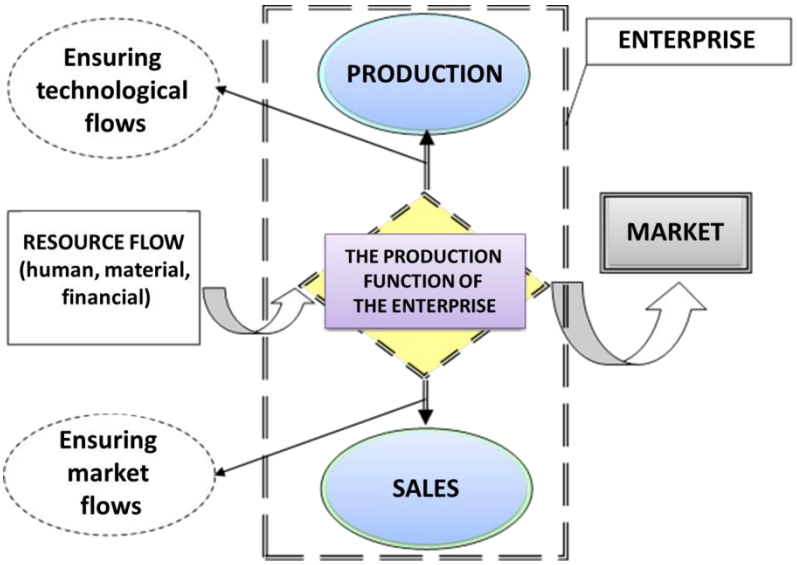

Fig. 6.10. The importance (place and role) of the production function in the enterprise-market circuit

Production management (PM) consists of all the activities of an organization and management of the industrial enterprise, activities carried out in order to efficiently achieve (profitably) as main function, namely the production function, which determines the main

object of activity of the enterprise. A strictly necessary (but not sufficient) condition for a efficient (profitable) realization of the production function of the enterprise is to give importance to the enterprise-market circuit. In a technological process (flow) of production, a certain technological stage transforms its own input quantities (resources) into output quantities (by-products, semi-finished products) for that technological stage.

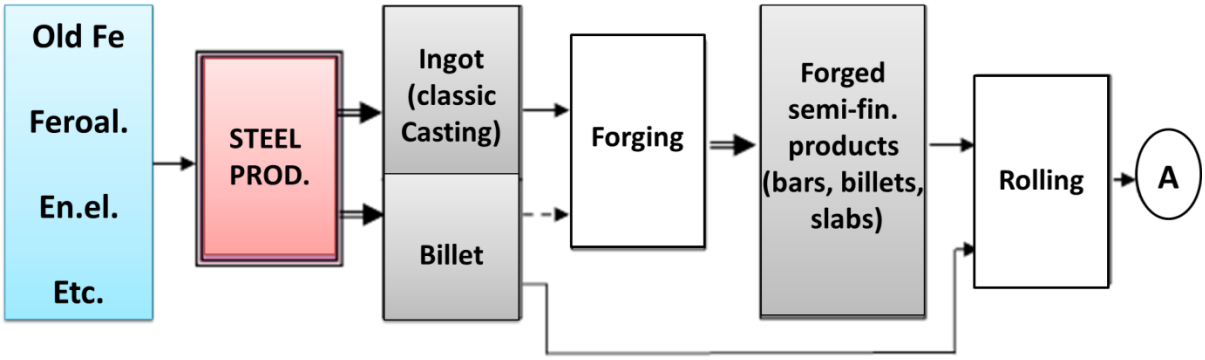

Fig. 6.13. Correlation and transformation of output quantities (by-products, semi-finished products) into input quantities (resources) for a production flow in the metal materials industry

The efficiency of production management is especially quantified by the level of customer satisfaction. In this sense, the production management must constantly take into account the basic requirements of any customer, namely: Quality (of P / L / S) maximum; optimal cost / quality input (usually minimum); Minimum production cycle (duration); Maximum flexibility (flexibility).

6.5. Conclusions

Researching the temporal evolution of the management concept, from the situational approach, then to the systemic approach, to the behaviorist (behavioral) approach and the traditional (classical) approach is very important to increase the efficiency of management principles and activities for any economic process with the main activity of producing non-ferrous alloys.

The correlation analyses between the managerial functions (forecasting, organization, coordination, command-training, evaluation-control) and the functions of the enterprise (personnel, financial, material, commercial, research-development-innovation) aim to be technologically, economically efficient and ecological process.

Chapter 7. THE INTERNATIONAL MARKET, PRODUCTION AND CONSUMPTION OF COMMON NON-FERROUS METALS IN THE PERIOD OF 2001-2021

This chapter starts with the argument that the production of metals in general and non-ferrous metals and alloys in particular is very important. In this context, a short history of non-ferrous metal production in Romania is also presented. An important aspect presented and analyzed in the paper is the evolution of aluminum production, consumption and price on the world market.

Given the great importance of metallic materials in the production of material goods with applications in various fields, at least now and in the near future, the maintenance or development of current living standards cannot be conceived without maintaining, developing and diversifying the production of metallic materials.

7.1. The production, consumption and price evolution of non-ferrous metals on the world market during 2019-2021

Prices for all non-ferrous metals fell sharply at the start of the 2020 pandemic, rising more than they did in 2021 in 2020. This growth is due to a strong recovery in China's economy, supply constraints and a weakening US dollar. In fig.7.22. the price of non-ferrous metals is presented, according to the London Metal Exchange (LME)

Tin had the highest rise, with a 113% increase on the London Metal Exchange (LME), compared to May 2021, followed by copper, which rose to a high of $ 10,417 per tonne, exceeding its previous peak of USD 10,160 per tonne in February 2011. Aluminum prices increased by 69% compared to 2020, compared to lead, nickel and zinc, which grew modestly by 46%, 36% and 49% per year, respectively.

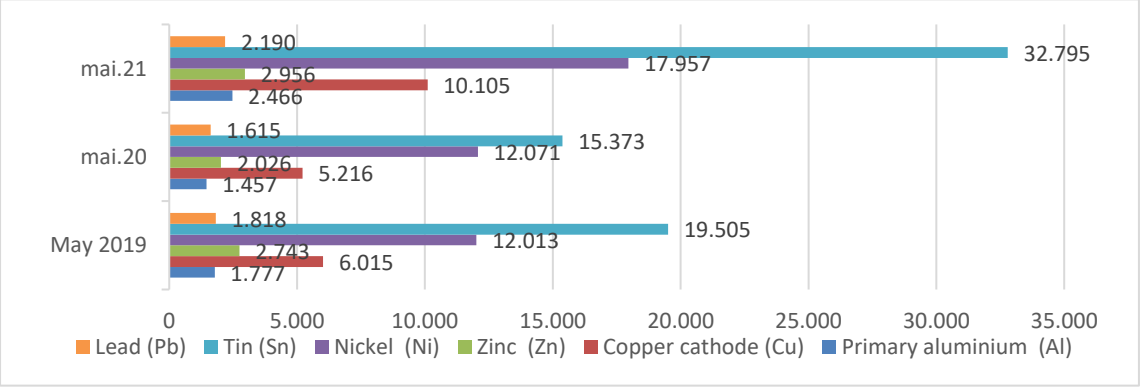

Fig.7.22. Non-ferrous metal prices according to London Metal Exchange (LME)

Global lead mine production is projected to increase by 5.1% to 4.75 million tonnes in 2021, while global demand is expected to increase by 3.9% in 2021 to 11.97 million. tons, ILZSG said.

Global supply of refined zinc is expected to exceed demand by 353,000 tonnes in 2021, the International Lead and Zinc Study Group (ILZSG) said on Friday, adding that global lead supply is expected to exceed demand by 96,000 tonnes (Reuters, April 30, 2021).

While copper, aluminum and tin saw an unprecedented rise in prices in 2020, zinc, lead and nickel saw only modest increases of 46%, 36% and 49% respectively. In the case of metallic zinc, the zinc market was in surplus in 2020 and is expected to remain in surplus this year as well.

7.2. Conclusions

The production, consumption and price economic analysis of common non-ferrous metals (Al, Cu, Pb, Zn and Ni) for the period 2001 - 2021 led to the following conclusions.

The main traditional producers of non-ferrous metals have maintained a relatively constant level of production, even though during this period many smaller operators have reduced or permanently stopped the production of non-ferrous metals. Of note is the unprecedented increase in non-ferrous metal production in China, which has become the world's largest producer of all metals analyzed;

The price of non-ferrous metals fluctuated sharply between 2001 and 2013. For all metals analyzed, the price recorded maximum values in the period 2005-2008, which coincides with the period of onset of the global economic and financial crisis. After 2008, prices have been on a downward trend and are currently fluctuating between 2006 and 2007, with the exception of copper, which had a record high of about $ 9,000 / t in 2011 and is currently on a slight downward trend.

The production, consumption and price economic analysis of common non - ferrous metals has highlighted large fluctuations in the international market in the context of the economic and financial crisis felt mainly in the countries of the European Union and in the United States. An important cause of fluctuations is the fact that non-ferrous metals are considered strategic metals and, in these conditions, demand and especially price, are particularly sensitive to both economic and political crises.

Chapter 8. BUSINESS PLAN FOR TIN AND LEAD-BASED ANTI-FRICTION ALLOYS

8.1. Objectives

Calcium and magnesium microalloyed anti-friction alloys obtained at **S.C. MELBA METALURGICAL SRL** prolongs the service life of machine parts, which makes the intervention of the human factor in their disassembly and assembly less often. When setting up the company, I took into account the fact that the company benefits from a superior technology for obtaining anti-friction alloys from raw metallic materials with a purity of 99.9%.

Based on these considerations, the main objective of the company is to obtain the YSn83 and YPbSn10 anti-friction alloys with improved characteristics by microalloying with calcium and magnesium.

8.2. Human resources

8.2.1. Leadership / management of the company

The leadership of the company will be performed by the manager of the company BUCIUMAN TEODOR, and the position of executive director is taken over by the administrator AVRAM VASILE, graduate engineer, with license and master's degree from the Faculty of Materials Science and Engineering, NON-FERROUS METAL ENGINEERING department.

The company **S.C. MELBA METALURGICAL SRL** will also have as employees:

- Economic director - 1 person;
- Engineer for analysis and quality control - 1 person;
- Worker - 2 people.

8.3. Marketing and sales plan

8.3.1. Product policy

The company **S.C. MELBA METALURGICAL SRL** aims to obtain anti-friction alloys YSn83 and YPbSn10 microalloyed with calcium and magnesium as final product.

Compared to the other anti-friction alloys on the market, the newly obtained anti-friction alloys, YSn83 and YPbSn10 microalloyed with calcium and magnesium, have several advantages, highlighted by the SWOT analysis:

The newly established company, with the objective of obtaining the anti-friction alloys YSn83 and YPbSn10 microalloyed with calcium and magnesium, has no competition in Romania. The company will have implemented a quality management system for non-ferrous alloys, according to STAS 202 and ISO 9001/2015 standards.

8.3.2. Distribution policy

The anti-friction alloys YSn83 and YPbSn10, microalloyed with calcium and magnesium, will be delivered directly to the beneficiary companies, at a date agreed between the manufacturer and the beneficiary.

8.3.3. *Advertisement policy*

The events organization and the company's presence on the Internet are two promotion strategies through which we want to make our products known. We set the promotion budget to be between 1000-5000 RON, depending on the promotion method.

8.3.4. Price policy

The obtained product being represented by new types of anti-friction alloys will be intended for use in rail transport, but also in the cement and energy industry.

The price of the product will be set based on costs and profit margin insurance. As far as competition is concerned, we will not take this into account, given that it is under-represented.

8.3.5. Target market segment

The quality of the productive activities is appropriate to be achieved through the use of machinery and equipment for high productivity and high precision. Productive activities will have to be carried out continuously, a situation that requires the existence of machinery and equipment, which will provide an operation without frequent interruptions of the activity, and in case of failure, the service time will be reduced to a minimum.

8.4. Operational analysis

8.4.1. Production / supply process

The production site will be in Pantelimon region, Ilfov County, on a leased area of 190 sqm. Rental costs: 4,750 lei / month.

8.4.2. Equipment, technology and facilities

TANGIBLE ASSET 1

In order to achieve the proposed objective, the company will purchase a spectrometer, a methane gas melting furnace, an electronic scale and a computer. The afferent furniture (2 desks, 2 executive chairs, etc.) will be purchased from IKEA; its value will not exceed 5,000 RON.

TANGIBLE ASSET 2

The car with which the product will be delivered will be the company's car, model Hyundai Tucson, B 213 MLB. As the business grows, it is intended to purchase another car which can be used by all employees, depending on the needs of the company.

FIXED INTANGIBLE ASSETS

The company S.C. MELBA METALURGICAL SRL will take all the necessary steps for ISO 9001-2015 certification.

The costs required for certification according to ISO 9001-2015 will include the hiring of a quality audit company, which will handle all the necessary documents. Estimated costs to achieve this target: EUR 1000. After obtaining this certification, as the company develops, the manager will take other steps to obtain a certification according to the STAS 202 standard.

8.5. Risk management

8.5.1. Risk identification

The risk is the possibility of losing or suffering prejudices as a result of future events that are currently uncertain. When we decide to invest in a business, the risks we take can have negative effects on the goals we set. Therefore, an analysis of all risk factors identified in this case will be performed.

8.5.2. Risk assessment

The risk assessment will be performed using the risk matrix. Following the identification and assessment of risks, it has been established that a number of measures are needed to reduce their risk tolerance.

It was found that the average risks which the company may face are related to the technology of obtaining the two alloys and the fluctuation of the purchase prices for the raw material, long delays in the delivery of raw materials. Given the fact that the company will produce new anti-friction alloys with a demand coming from important branches of industry, any delay in the delivery of raw materials or disruption of technological flow will affect the company's image.

8.6. Business plan budget

The annual budget was based on previously estimated costs.

8.7. Applicability of the business plan / Sustainability in relation to the field of study

I consider that the business plan is opportune, because the chosen research topic, "Improving the characteristics of YSn83 and YPbSn10 anti-friction alloys by calcium and magnesium microalloying", represents a domain of great interest for rail transport but also for the cement and energy industry.

Business sustainability

In order to ensure the sustainability of the business, definitive measures will be considered according to the 3 pillars: environmental, social and economic.

8.8. Social innovation

The proposed business aims to obtain the anti-friction alloys YSn83 and YPbSn10 by microalloying with calcium and magnesium. The alloys thus obtained prolong the service life of the machine parts, which makes the intervention of the human factor in their disassembly and assembly less often. I believe that the company's involvement in obtaining these anti-friction alloys has a beneficial effect on many branches of industry, contributing to increasing the reliability and maintenance of machines / equipment / industrial installations, this being reflected in the increasing in quality and security of life.

Chapter 9. CONCLUSIONS AND PERSONAL CONTRIBUTIONS

9.1.Conclusions

Significant improvement of the tribological properties of the classic anti-friction Sn-based alloys (Babbitt alloys) and Pb-based alloys is obtained by microalloying with additional elements such as As, Cd, Ni, Cr, Al, Mn, Te, Pb (in Sn alloys), etc.

Out of these, As and Cd gave the best results, despite their toxicity for health and the environment. The legislation of using of such elements in various applications has also led to studies and research in the case of anti-friction alloys to find substitutes, such as: Li, Na, Tl, In, Ga, Tr, etc.

Two anti-friction alloys were obtained, YSn83 and YPbSn10. The obtained alloys were subsequently microalloyed with Mm in the amount of 0.1, 0.2, 0.5 and 1wt. %. The alloys obtained were characterized from a microstructural point of view. The chemical analyzes performed confirmed the initial composition.

For Ysn83 alloys, a slightly modified microstructure can be observed at the addition of 0.1% Mm and completely different at 1 wt. % concentration of Mm. We can mention that the sample with 0.2% Mm has a more homogeneous microstructure and with less segregated compounds than the sample with 0.5% Mm. For the 1% Mm sample we can also see that the Cu_6Sn_5 compound has been highlighted but SnSb is missing.

For YPbSn10 alloys, the polyhedral SnSb crystals are predominantly observed in all the samples obtained, except for the 1wt. % Mm alloy, which has predominantly acicular crystals with the microstructure radically modified compared to the base alloy.

The melting-alloying equipment used for the production of these alloys was patented by the author for composite materials but it was successfully used for the production of anti-friction alloys alloyed with misch metal. Its use has reduced the production time of Mm microalloyed anti-friction alloys.

For the rare earth (mish metal) microalloyed YSn83 and YPbSn10 samples it was found that the increase of the hard phase dispersion in the soft matrix of the alloys may be the consequence of the increase in the HB hardness of the alloys by 3-5% and the compressive strength by 3-6 %. It was also been observed that, as the temperature rises, the hardness decreases, as a consequence of possible recrystallization phenomena that occur during the samples heating; it is known that Sn and Pb alloys have relatively low recrystallization temperatures.

Three relatively evenly distributed compounds have been identified in the metal matrix of Sn alloys. The first compound has elements of trigonal symmetry; the second compound is irregular in shape embedding the first one and the third compound having acicular-columnar shape. The compound with elements of trigonal symmetry acts as a crystallization germ for the irregularly shaped compound.

EDS point semiquantitative chemical analyzes performed on each structure indicate the following chemical composition:

- the trigonal compound contains mostly Sb-Cu-Mg
- the irregularly shaped compound contains mostly Sb-Sn

- the compound with acicular-columnar shape, contains mostly Cu-Sb-Sn

A distribution of the elements according to each structure was obtained using EDS / live-map analysis.

For the YS1 and YS2 samples we can observe a similarity of the diffractograms, the high peak containing Ca for the YS1 sample and Mg for the YS2 sample. Also, the middle peak which corresponds to the two diffractograms is represented by the compound Cu_6Sn_5. For the rest, there are small differences due to the effect of the used microalloying elements.

For the processing of the collected experimental data, the following aspects were taken into account:

- The background (viewed as information contained in the data collected) was removed from the qualitative phase analysis.

- The Kα2 component has been removed.

In the case of samples YP1 and YP2, the X-ray diffraction analysis highlights the presence of a majority phase of solid solution type with Pb base, solid substitution solution and a SnSb compound with rhombohedral structure. The analysis also identifies a small percentage of Cuprostibite in the case of the first sample.

In the case of samples YS1 and YS2, the presence of a majority tetragonal structure is observed, associated with βSn. The analysis of the results shows the lowest values of the coefficient of friction were obtained for the YS2 sample. In the case of this test, the increase in relative slip velocity does not significantly affect the coefficient of friction values. Only an increase in the normal loading force leads to a slight increase in the coefficient of friction.

9.2. Personal contributions

In the first part of this doctoral thesis, I did a comprehensive theoretical study to substantiate the existing notions for these anti-friction alloys that will be used for tribological applications.

I achieved the alloying with rare earths (0.1%, 0.2%, 0.5% and 1% mischmetal) of the YSn83 alloy in an original installation.

I studied the microstructure of the obtained alloys and I studied the hardness and compression behavior of the alloys obtained at different temperatures.

I made the microalloying with rare earths (mischmetal) in percentages of 0.1%, 0.2%, 0.5% and 1% of the YPbSn10 alloy.

I studied the microstructure and mechanical properties of the obtained alloy.

I obtained original compositions of YSn83 alloy microalloyed with 0.2% Ca and 0.2% Mg.

I obtained original compositions of YPbSn10 alloy microalloyed with 0.2% Ca and 0.2% Mg.

I did an extensive structural study of the obtained alloys.

I performed tribological analyzes to identify the behavior of antifriction alloys microalloyed with Ca and Mg.

The results obtained showed a significant improvement in the structure of YSn83 alloys microalloyed with Mg.

For YPbSn10 alloys microalloyed with Ca, the best tribological tests results were obtained.

Related to the second part of the doctoral thesis, I presented viable solutions in the field of management of non-ferrous metals and alloys, studying the market, production and evolution of non-ferrous metals costs in order to achieve a business plan and a marketing plan to place on the national and international market the patented anti-friction materials.

In this case:

- I have created a managerial structure intended to companies that are producing non-ferrous metallic materials,
- I performed an economic analysis of the production costs, consumption and price of common non-ferrous metals (Al, Cu, Pb, Zn and Ni) for the period 2001 - 2021
- I developed a business plan, designed to develop a new company to sell anti-friction alloys, according to the conducted studies from the doctoral thesis, based on which two CBI were submitted to OSIM, a business plan was made according to the requirements of the financial-banking market.

I will continue my research, in a POSTDOC scholarship or on my own, on the production of anti-friction alloys from powders, alloyed with rare earths (lanthanum, cerium, praseodymium, neodymium, promethium, samarium, europium, gadolinium, terbium, dysprosium, holmium, erbium, thulium, ytterbium lutetium, and yttrium). To this end, I will look for cheap, widely available, cost-effective types of raw materials to create anti-friction materials capable of ensuring the reliability, durability and high performance of friction units, especially in difficult working conditions. In addition, such materials should be made using simple technology and cheap raw materials, which do not directly pollute the ecosystem and the biosphere, with pollution being an acute problem on a global scale.

The original results of this doctoral thesis were the subject of 2 scientific articles, published in ISI JOURNALS (Web of Science) and 1 published in the International Specialized Journal MATERIALS, listed Q1 (red zone), with impact factor 3,623, 3 oral communications at international scientific events, listed ISI, 2 Patent Applications, registered at OSIM and 2 posters presented at the INVENTCOR 2021 International Invention Show, where I obtained 2 GOLD medals, 2 TROPHIES and afferent diplomas.

REFERENCES (Selections)

[1] Vasilică Gh., Bită O. (1967), Procese de lubrificație, frecare și uzură la suprafețele metalice, Ed. Academiei RSR, București

[2] Mang T., Bobzin K, Bartels T. (2011), Industrial Tribology. Tribosystems, Friction, Wear and Surface Engineering, Lubrication, WILEY-VCH Verlag & Co. KGaA, Germania

[3] Ludema K.C. (1996), Friction, Wear, Lubrication, A Textbook in tribology, CRC Press LLC, SUA, Chapter 7: Metallic antifriction materials, p.223-254.

[4] Manea Gh. (1970), Organe de mașini, vol.1. Ed.Tehnică, București, Capitolul Lagăre cu alunecare, p.735-347

[5] Guruswamy S. (2000), Engineering properties and applications of lead alloys, Marcel Dekker Inc., NY SUA

[6] Glaeser W.A. (1992), Materials for tribology, Elsevier Science Phblishers B.V. Amsterdam, Olanda

[7] Habashi F (Editor), (1998), Alloys - Preparation, Properties, Applications, ISBN 3-527-29591-7, WILEY-VCH Verlag GmbH, D-69469 Weinheim, Germania

[8] Matucha K.H. (Vol. Ed.) (1996), Structure and Properties of Nonferrous Alloys, ISBN: 3-527-26821-9, WILEY-VCH Verlag GmbH, D-69469 Weinheim, Germania

[9] Ienciu, M., Moldovan, P., Panait, N., Buzatu, M., - Elaborarea și turnarea aliajelor neferoase, Editura Didactică și Pedagogică, București, 1982.

[10] T. B. Majdanczuk, W. M. Iljuszenko, A. N. Bondarenko (2017), Effect of Modifying and Alloying Elements on the Structure and Properties of Surfaced Layers Made of High-Tin Bronze, Biuletyn Instytutu Spawalnictwa No. 1, pp. 39-43

[11] Șontea S. et.al. (1981), Metale și aliaje neferoase de turnătorie, Ed.Scrisul românesc, Craiova, România

[12] Popescu, V. I (1967), Tehnologia forjării și extruziunii, Editura didactică și pedagogică, București

[13] Han Q. (Ed), (1998), Rare Earth, Alkaline Earth and Other Elements in Metallurgy, IOS Press, Amsterdam, Olanda

[14] I. Yu. Efimochonkin, S. B. Lomov, I. E. Goncharov, S. V. Fedotov, 2008, Patent RF 2436857, Powder composite material.

[15] S.N. Grigoriev, M.A. Volosova, Application of coatings and surface modification of the tool: Textbook. allowance. - Moscow: MSTU "Stankin": Janus-K, 2007. pp 342.

[16] M.A. Zlensko, M.V. Nogaitzev, V.M. Dovbysh, Additive technologies in mechanical engineering. Lambert Academic Publishing, 2015. Pp 224

[17] Brevet RO132816-B1, Procedeu si instalatie de obtinereelectrochimica a unui material compozit cu matrice metalica, Inventatori: ARGHIRESCU M,COSTOIU M C, SEMENESCU A, **AVRAM Vasile**, BURADA M, MILITARU N G, AMZA C G, CHIVU O

[18] **Vasile Avram**, Augustin Semenescu, MISCH METAL MICRO-ALLOYING EFFECT ON MECHANICAL PROPERTIES OF BABBITT ALLOYS, U.P.B. Sci. Bull., Series B, Vol. 83, Iss. 2, 2021 ISSN 1454-233, pp. 221 – 230

[19] **Vasile Avram**, Augustin SEMENESCU, Ioana CSÁKI, Y-PbSn10 ANTIFRICTION ALLOYS MICROALLOYED WITH MISCHMETAL, U.P.B. Sci. Bull., Series B, Vol. 83, Iss. 4, 2021 ISSN 1454-2331, pp. 307 – 312

[20] Brevet A202100494 Alloys for tribological applications **AVRAM Vasile**, SEMENESCU Augustin, CSÁKI Ioana, STOICA Alina Maria, University Politehnica Bucharest

[21] Brevet A202100495 Antifriction alloys improved by microalloying **AVRAM Vasile**, SEMENESCU Augustin, CSÁKI Ioana, STOICA Nicolae Alexandru, University Politehnica Bucharest

[22] **Vasile AVRAM**, Ioana CSÁKI, Ileana MATES, Nicolae Alexandru STOICA, Alina-Maria STOICA Augustin SEMENESCU, *The Effect of Ca and Mg on the Microstructure and Tribological Properties of YPbSn10 Antifriction Alloys*, **Materials 2022, Volume 15, Issue 9, 3289., Metals and Alloys, Structure and Mechanical Properties of Alloys II**, pag.1-10, **IF 3,623, Quartile Q1 (zona roșie)**, https://doi.org/10.3390/ma15093289, www.mdpi.com/journal/materials

[23] **Vasile AVRAM**, Augustin SEMENESCU, Adrian IOANA, Resit UNAL, Dragoș MARCU, EVOLUTION OF NON-FERROUS METALS PRODUCTION, CONSUMPTION AND PRICE ON THE WORLD MARKET IN THE THIRD MILLENIUM, The 10th International Conference of Management and Industrial Engineering Business Change and Digital Transformation in a World Moving Through Crisis" ICMIE 2021, November 11th– 13th, 2021, https://www.icmie-faima.ro/

[24] Adrian IOANA, **Vasile AVRAM**, Augustin SEMENESCU, MANAGEMENT ELEMENTS APPLICABLE IN THE PRODUCTION OF NON-FERROUS ALLOYS, The 10th International Conference of Management and Industrial Engineering Business Change and Digital Transformation in a World Moving Through Crisis" ICMIE 2021, November 11th– 13th, 2021, https://www.icmie-faima.ro/